frontiers | Frontiers in Earth Science

TYPE Original Research
PUBLISHED 23 September 2022
DOI 10.3389/feart.2022.1011219

OPEN ACCESS

EDITED BY
Hu Li,
Southwest Petroleum University, China

REVIEWED BY
Haiyan Wu,
Chang'an University, China
Li Keyong,
Xi'an University of Science and Technology, China
Guo Yanqin,
Xi'an Shiyou University, China

*CORRESPONDENCE
Xinming Sun,
296027311@qq.com
Xuejiao Yuan,
yxjxx21@163.com

SPECIALTY SECTION
This article was submitted to Structural Geology and Tectonics, a section of the journal Frontiers in Earth Science

RECEIVED 03 August 2022
ACCEPTED 22 August 2022
PUBLISHED 23 September 2022

CITATION
Wei X, Sun X, Yuan X and Yang Y (2022), Characteristics and prediction of permian tight glutenite reservoirs in dinan 15 well block, junggar basin. *Front. Earth Sci.* 10:1011219. doi: 10.3389/feart.2022.1011219

Characteristics and prediction of permian tight glutenite reservoirs in dinan 15 well block, junggar basin

Xin Wei[1], Xinming Sun[1]*, Xuejiao Yuan[2,3]* and Yiming Yang[2,3]

[1]Karamay Vocational & Technical College, Karamay, China, [2]School of Geoscience and Technology, Southwest Petroleum University, Chengdu, China, [3]Natural Gas Geology Key Laboratory of Sichuan Province, Southwest Petroleum University, Chengdu, China

Glutenite reservoirs are characterized by rapid lateral change, strong heterogeneity, and complex main controlling factors. This research aims to identify macro and micro characteristics of glutenite reservoirs and establish criteria for identifying favorable reservoirs studies. To this end, the tight sandy conglomerate of the Upper Wuerhe Formation in the Permian Upper Wuerhe Formation in the Dinan 15 well area of the eastern slope of the Dongdaohaizi sag in the Junggar Basin is studied. The core observation, physical property analysis, sensitivity analysis, casting thin section, scanning electron microscope and logging data are adopted to comprehensively analyze the characteristics of glutenite reservoirs. By integrating various reservoir characteristic parameters, this work constructed a new set of reservoir evaluation criteria to predict favorable areas for the Upper Wuerhe Formation in Dongdaohaizi Sag. The results show that the lithology of the Upper Wuerhe Formation in the Dinan 15 well area is dominated by gray glutenite; the reservoir is an ultra-low porosity and ultra-low permeability reservoir with moderately weak water sensitivity and weak velocity sensitivity. The reservoir space types of the layers are mainly intergranular pores; the shape of the mercury intrusion curve and the pore throat radius distribution of the samples show that the reservoir is skewed, poorly sorted, and has the characteristics of small pores and thin throats. This work constructed evaluation criteria for reservoirs from I to III by utilizing lithology, physical properties, sensitivity, reservoir space type, and microstructural characteristics as key parameters. The favorable reservoir distribution area is mainly located in the west of the block, which is the focus of the next exploration of the Upper Wuerhe Formation area. The research results improved understanding of glutenite reservoir characteristics and will serve as significant guidance for the oil and gas exploration in the Dinan 15 well area.

KEYWORDS

reservoir characteristics, reservoir prediction, upper wuerhe formation, permian, dongdaohaizi sag, junggar basin, glutenite reservoirs

1 Introduction

Glutenite reservoirs are characterized by rapid lateral change, strong heterogeneity, and complex main controlling factors. Classifying their quality and predicting productivity are difficult, which have become a research hotspot in recent years (Jin et al., 2022). Glutenite reservoirs result from the deposition of near-source sediment and the mixed accumulation of coarse components such as sand and gravel (Qu et al., 2017; Lin et al., 2019; Pang et al., 2020). The complexity of the reservoir makes it difficult to select and evaluate high-quality glutenite reservoirs, and traditional qualitative and quantitative analyses are limited in this regard (Qu et al., 2017). At present, most studies on glutenite reservoirs focus on petrology, sedimentology, pore structure, etc., (Liu et al., 2018; Bian et al., 2020; Yang et al., 2020). Few studies have explored how reservoir capabilities affect fluids and the sensitivities of both acidity and alkalinity from the perspective of reservoir sensitivity. Besides, China has achieved breakthrough regarding oil and gas exploration in the glutenite reservoirs in Junggar Basin, Bohai Bay Basin, Songliao Basin, Erlian Basin, etc., (Wang et al., 2020a; Zhou et al., 2020; Hu et al., 2021a; Hu et al., 2021b; Lu et al., 2021). The oil and gas exploration in the representative Permian-Triassic glutenite reservoirs in Junggar Basin is so groundbreaking that it has become the current research focus of petroleum geology(Kuang et al., 2014; Zhi et al., 2018) Up to now, many large-scale oil and gas reservoirs containing glutenite as reservoirs have been identified in the Permian strata of the Junggar Basin, especially the identification of the billion-ton-grade glutenite reservoirs of oil and gas in the Baikouquan Formation, Mahu Sag, Junggar Basin, which has promoted the general research in the Permian and Triassic glutenite reservoirs in Junggar Basin (Zhi, 2016; Li et al., 2018; Xiao et al., 2019; Hu et al., 2020; Li, 2022). New progress in oil and gas exploration was realized in the glutenite reservoirs of the Permian Upper Wuerhe Formation of Shawan Sag, Dongdaohaizi Sag and Fukang Sag after the identification of the glutenite reservoirs in the Triassic Baikouquan Formation of Mahu Sag, further proving the magnificent exploration potential of glutenite reservoirs (Du et al., 2019; Zhao et al., 2019; Li et al., 2020; Gao, 2021; Guan et al., 2021). Additionally, Dongdaohaizi Sag is one of the important hydrocarbon-rich sags of the Junggar Basin, while the Permian Upper Wuerhe Formation has developed fan-delta glutenite reservoirs and is the important oil-bearing series of Dongdaohaizi Sag since it is close to the source rocks of the underlying Pingdiquan Formation and has developed faults connected with source rocks (Zhang, 2014; Jin et al., 2015).

The oil and gas exploration in Dongdaohaizi Sag with the Pingdiquan Formation as the source began from the 1990s until relatively significant breakthrough was realized in oil and gas exploration in 2013 when the glutenite reservoirs of the Upper Wuerhe Formation DN8 Well were deployed by following the idea of "separating blocks and controlling reservoirs", but a series of exploration of preliminary prospecting wells and appraisal wells that was deployed sequentially failed to achieve satisfactory results. According to the research of fine sedimentary paleogeomorphology (Zou et al., 2016; Xu et al., 2017; Cai et al., 2019; Wang et al., 2022), the Permian Upper Wuerhe Formation is regressive fan delta sedimentation, with wide distribution of favorable facies zones in the fan delta front. In 2019, DN14 and DN15 wells were deployed in the optimal favorable facies zones of the Upper Wuerhe Formation fan delta front, resulting in highly productive hydrocarbon flow, which is the evidence of the magnificent exploration potential of the Upper Wuerhe Formation, Dongdaohaizi Sag. Since the Upper Wuerhe Formation has been cumulatively influenced by multi-stage tectonic movement, featuring complex geological characteristics, the glutenite reservoirs and their prediction need to be further studied (Qu et al., 2017; Hu et al., 2021a).

According to previous studies, the porosity and permeability of a glutenite reservoir is generally less than 10.0% and 5.000 mD, respectively, featuring low porosity and permeability (Liu, 2015; Xu et al., 2017; Li et al., 2019; Wang et al., 2022), and is a near-source melange sedimentary system, with complex lithological compositions, diverse textures and structures of rocks, and frequent change in plane characteristics of lithofacies (Zou et al., 2016; Jin et al., 2017; Jin et al., 2022). Since diagenesis and pore evolution have critical influence over the physical characteristics of reservoirs (Fu et al., 2019; Lin et al., 2019), the characteristics of the glutenite reservoirs of the Permian Upper Wuerhe Formation on the eastern slope of Dongdaohaizi Sag, Junggar Basin have been researched to some extent, but studies like general analysis and classified evaluations on the characteristics of favorable reservoirs and through based on various characteristic parameters of reservoirs are quite rare. The study in this paper took the Permian Upper Wuerhe Formation on the eastern slope of Dongdaohaizi Sag, Junggar Basin as the example, and carried out a prediction of favorable areas of the Upper Wuerhe Formation in Dongdaohaizi Sag through a general analysis on the glutenite reservoir characteristics in combination with various parameters of reservoir characteristics using core observation, physical characteristic analysis, sensitivity analysis, casting thin section, scanning electronic microscopy (SEM), well logging, etc., in the hope of providing guidance for the exploration and development of the tight glutenite reservoirs in the area mentioned hereinabove.

2 General geological situation

Junggar Basin, located in the western China, is a typical large-scale hydrocarbon-bearing superimposed sedimentary basin in the western China (Yang et al., 2020; Zhang et al., 2021), with the geographic coordinates of E81°C–92°C, N43°C–48°C. It is

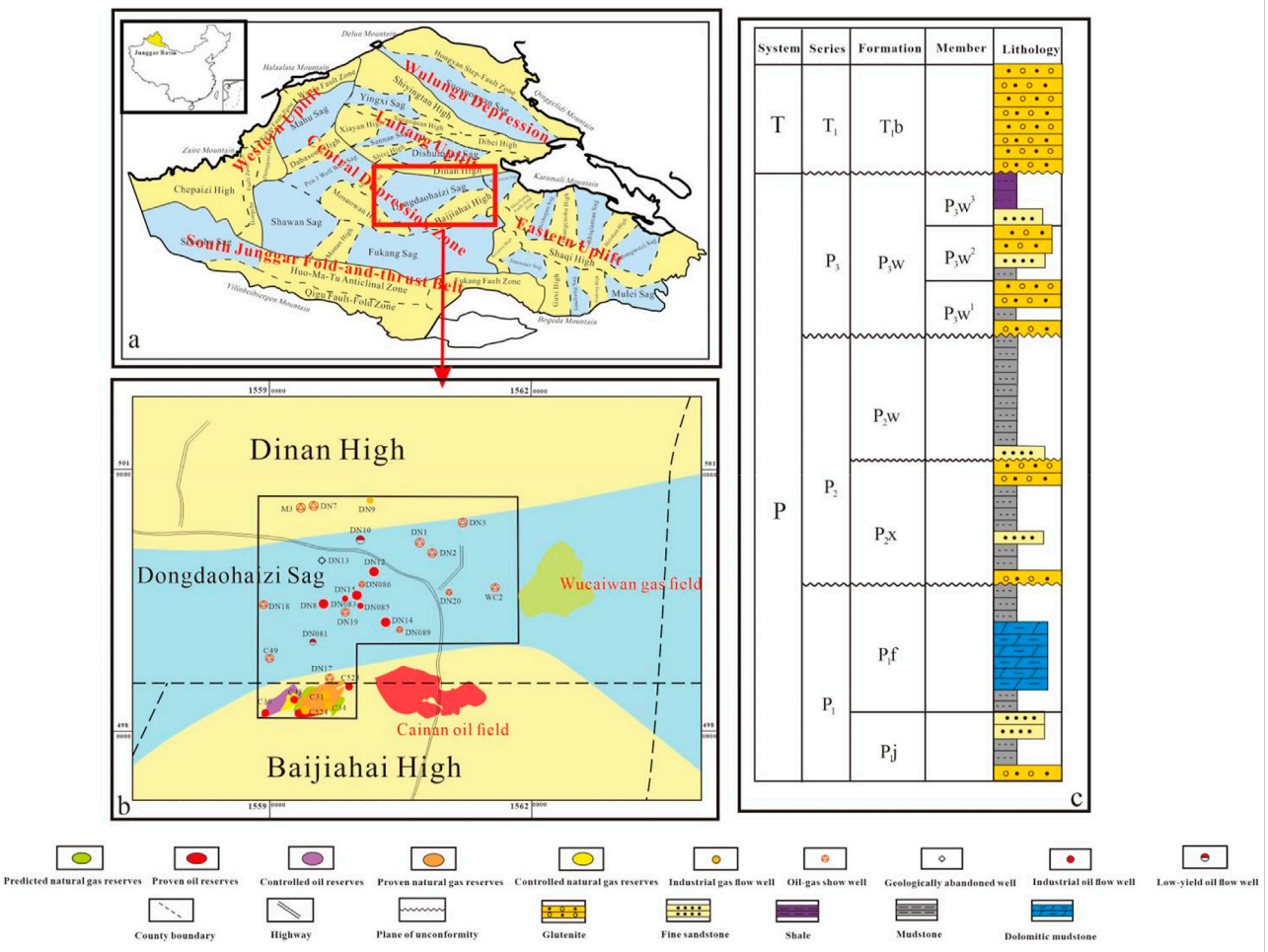

FIGURE 1
Basic regional pattern and comprehensive stratum column chart of study area. **(A)** Geographic location and Paleogene structure block plan of Dongdaohaizi Sag of the central depression, Junggar Basin; **(B)** Location of the Dinan 15 well in the study area; **(C)** Comprehensive column chart of the Upper Permian series, Junggar Basin.

surrounded by fold mountain systems, with the Hala'alat Mountain and the Zaire Mountain to the northwest, the Altai Mountain and the Kelameili Mountain to the northeast, and the northern Tianshan Mountains to the south. The plane shape of the basin is an approximate triangle, wide in the south and narrow in the north, about 700 km from west to east and about 370 km from north to south, with an area of 13.6×10^4 km^2. Junggar Basin consists of multiple tectonic units, including 6 primary tectonic units, i.e., Wulungu Sag, anteclise uplift, central depression, eastern uplift, western uplift, and northern Tianshan piedmont thrust, which can be further classified as 44 secondary tectonic units (Zhang, 2019; Zhang et al., 2020a; Zhang et al., 2022a; Zhang et al., 2022b).

Dongdaohaizi Sag, located in the northeast of the central depression of Junggar Basin, is between the Dishuiquan fault zone and the northern Dongdaohaizi fault zone, extending in a belt shape along the northeast-southwest direction and covering an area of 7,000 km^2 or so (Figure 1A). It is paleogeomorphologically an asymmetric double-fault graben-like sag and has a relatively simple internal structure, which is dominated by traction hook-shaped low-amplitude structures of downthrown blocks of faults. Dongdaohaizi Sag starts from the southern Dishuiquan fault and the Dinan uplift in the north, connected with the Baijiahai fault and the Baijiahai uplift in the south, bounded with No. 1 and 2 Faults of the northern Mosuowan, the Mosuowan uplift, and the northern Mosuowan uplift in the west, and connected with Wucaiwan Sag in the east (Ding, 2016; Zhang et al., 2022c; Zhang et al., 2022d). Additionally, the strata of Dongdaohaizi Sag are relatively completely developed, consisting of limestone stratum, Permian stratum, Triassic stratum, Jurassic stratum, Cretaceous stratum and Cenozoic stratum distributed from top

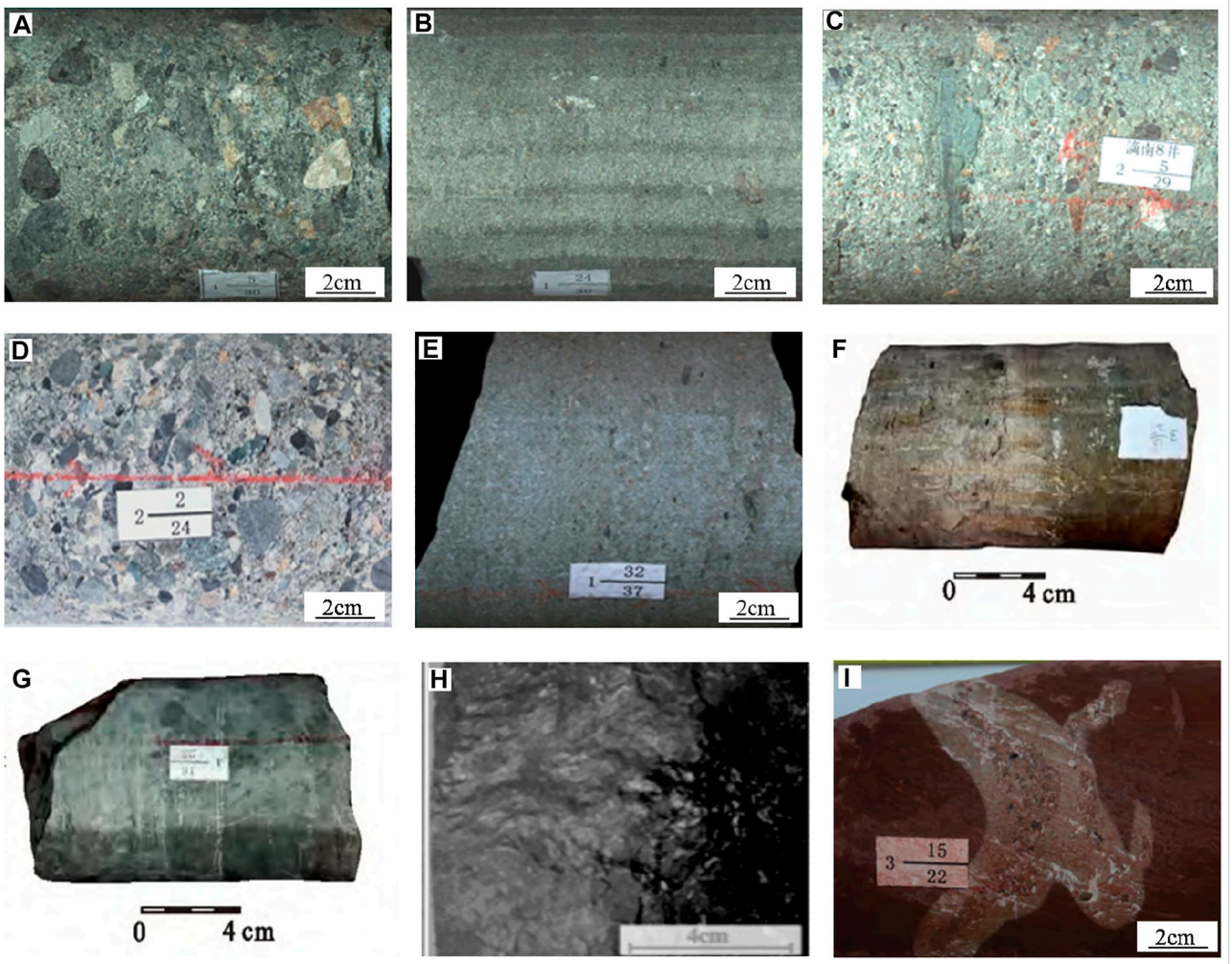

FIGURE 2
Basic lithological characteristics of the Upper Wuerhe Formation in the study area. **(A)** Glutenite, Dinan 19 well, P_3w_1, 3,922.37 m–3,922.52 m; **(B)** Pebbly sandstone, Dinan 19 well, P_3w_1, 3,922.37 m–3,922.52 m; **(C)** Glutenite, Dinan 15 well, P_3w_2, 3,732.99 m–3,733.17 m; **(D)** Glutenite, Dinan 15 well, P_3w_2, 3,792.18 m–3,792.36 m; **(E)**. Pebbly sandstone, Dinan 15 well, P_3w_2, 3,738.56 m–3,738.65 m; **(F)** Medium–fine sandstone, J202 well -13/27 (Zou et al., 2021); **(G)** Mudstone, siltstone, K82 well 4–16/26(Zou et al., 2021); **(H)** Brown mudstone, MH014 well, 3,736.98 m(Zhang et al., 2020b); **(I)** Mudstone, Dinan 11 well, P_3w_3, 4,603.63 m–4,603.81 m(Hu et al., 2021b).

to bottom. Among them, the Permian stratum has developed the Xiazijie Formation, the Lower Wuerhe Formation and the Upper Wuerhe Formation (Figure 1C). The early–middle Permian is the sag-filling sedimentation stage, and the Xiazijie Formation (P_2x) is a set of significantly thick greyish brown and brownish grey glutenite mixed with minor grey and brownish grey mudstone and sandstone. The Lower Wuerhe Formation (P_2w) is a set of grey and dark grey mudstone and sandy mudstone mixed with greyish green and brownish grey glutenite and lime mudstone. The dark mudstone rich in alga has formed the high-quality source rocks close to the source reservoirs of Dongdaohaizi Sag. Vertically, the contact between the Upper Wuerhe Formation and the overlying Baikouquan Formation is unconformable, so is the contact between the Upper Wuerhe Formation and the underlying Lower Wuerhe Formation (Feng, 2017; Wang J. et al., 2020; Li, 2022). The Upper Wuerhe Formation has developed large-scale regressive fan delta sedimentation, while the thick-bedded sandstone of the Wuerhe Formation Section I, the thin-bedded sandstone of the Wuerhe Formation Section II and the mudstone of the Wuerhe Formation Section III have formed a good reservoir cap combination and provide excellent geological conditions for the formation of large-area lithology-strata hydrocarbon reservoirs. In the study area of this paper, the regional structure of the Dinan 15 well block, located on the eastern slope of Dongdaohaizi Sag of the central depression, Junggar Basin, is administratively governed by Fuhai County, Altay Prefecture, Xinjiang Uygur Autonomous Region, about 6 km to the Cainan oilfield in the south, about 24 km to the

TABLE 1 Classification standard for physical characteristics of clastic rock reservoirs (by national reserves committee, 1997).

Reservoir classification	Porosity Φ(%)	Permeability K(× 10 μm$^{2-3}$ μm^2)
Super-high porosity and high permeability	$\Phi \geq 30$	$K \geq 2000$
High porosity and permeability	$25 \leq \Phi < 30$	$500 \leq K < 2000$
Medium porosity and permeability	$15 \leq \Phi < 25$	$50 \leq K < 500$
Low porosity and permeability	$10 \leq \Phi < 15$	$5 \leq K < 50$
Super-low porosity and low permeability	$\Phi < 10$	$K < 5$

Wucaiwan gas field in the east, and about 18 km to the Dishuiquan oilfield in the northeast (Figure 1B). The earth surface in this area is desert, with flat terrain, and has a ground elevation of 670 m–705 m and an average ground elevation of 691.7 m.

3 Fine-grained sedimentary rock reservoir characteristics

3.1 Lithological characteristics

The Upper Wuerhe Formation can be divided into three sections, i.e., P_3w_1, P_3w_2, and P_3w_3 from top to bottom. According to the photos of the cores from the Upper Wuerhe Formation, the lithology of P_3w_2 and P_3w_1 of the Upper Wuerhe Formation is respectively dominated by glutenite, followed by pebbly sandstone (Figure 2). Among the two sections, the Upper Wuerhe Formation P_3w_1 features fan delta plain facies and is lithologically dominated by grey glutenite, mixed with thin-bedded silty mudstone, poor in reservoir characteristics, and 50 m–110 m thick, while the Upper Wuerhe Formation P_3w_2 features fan delta front facies and is lithologically dominated by grey glutenite and interbedding of pebbly sandstone and brown mudstone, and thus is the main section of high quality reservoir development, with the thickness of 110 m–150 m.

3.2 Physical characteristics

In order to identify the physical characteristics of the Upper Wuerhe Formation glutenite reservoirs, analysis was conducted on 420 samples of Section II, the Upper Wuerhe Formation and 204 samples of Section I, the Upper Wuerhe Formation both collected from Dinan 15 well. The reservoir porosity and permeability of Section I, the Upper Wuerhe Formation are generally less than 8% and lower than 2.56 μm^2 × 10^{-3} μm^2, respectively, while those of Section II, the Upper Wuerhe Formation are generally less than 12% and lower than 5 × 10^{-3} μm^2, respectively. According to the classification standard for physical characteristics of clastic rock reservoirs (Table 1), generally speaking, the Upper Wuerhe Formation reservoirs in the study area are classified as super-low porosity and permeability reservoirs (Liu, 2015; Kang et al., 2019; Huang et al., 2020; Xiao et al., 2020).

According to the histograms of porosity and permeability of Section I, the Permian Upper Wuerhe Formation of Dinan 15 well (Figures 3A–D), the range, median and average of the porosity of 74 reservoir samples from Section I, the Upper Wuerhe Formation are 2.2%–11.6%, 4.61%, and 4.95%, while the range, median and average of the permeability of 65 reservoir samples from the same section are 0.01 μm^2–2.33 μm^2 × 10^{-3} μm^2, 0.028 μm^2 × 10^{-3} μm^2 and 0.058 μm^2 × 10^{-3} μm^2, respectively. Therefore, the reservoirs in this section feature super-low porosity and permeability. The range, median and average of the porosity of 35 oil reservoir samples are 5.0%–11.6%, 5.54% and 6.10%, respectively, while the range, median and average of the permeability of 30 oil reservoir samples are 0.016 μm^2~.33 μm^2 × 10^{-3} μm^2, 0.057 μm^2 × 10^{-3} μm^2, and 0.117 μm^2 × 10^{-3} μm^2, respectively. As shown in the histograms, the porosity of Section I, the Permian Upper Wuerhe Formation of Dinan 15 well is mostly less than 8% and its permeability is all below 2.56 μm^2 × 10^{-3}μm^2. Therefore, this section has poor physical characteristics and features typical super-low porosity and low permeability (Xiao et al., 2019).

The value distribution of porosity and permeability between every section is significantly different. According to the histograms of porosity and permeability of Section II, the Permian Upper Wuerhe Formation of Dinan 15 well (Figure 3E–H), the range, median and average of the porosity of 138 reservoir samples from Section II, the Upper Wuerhe Formation are 2.3%–17.2%, 6.89%, and 7.05%, respectively, while the range, median and average of the permeability of 124 reservoir samples from the same section are 0.01 μm^2–939 × 10^{-3} μm^2, 0.145 μm^2 × 10^{-3} μm^2, and 0.311 μm^2 × 10^{-3} μm^2, respectively. The range, median and average of the porosity of 85 samples are 5.2%–17.2%, 7.71%, and 8.25%, respectively, while the range, median and average of the permeability of 73 samples are 0.067 μm^2–939 μm^2 × 10^{-3} μm^2, 0.663 μm^2 × 10^{-3} μm^2, and 1.626 μm^2 × 10^{-3} μm^2, respectively. As shown in the histograms, the porosity of Section II, the Permian Upper Wuerhe Formation of Dinan 15 well is mostly less than 12% and its permeability is mostly

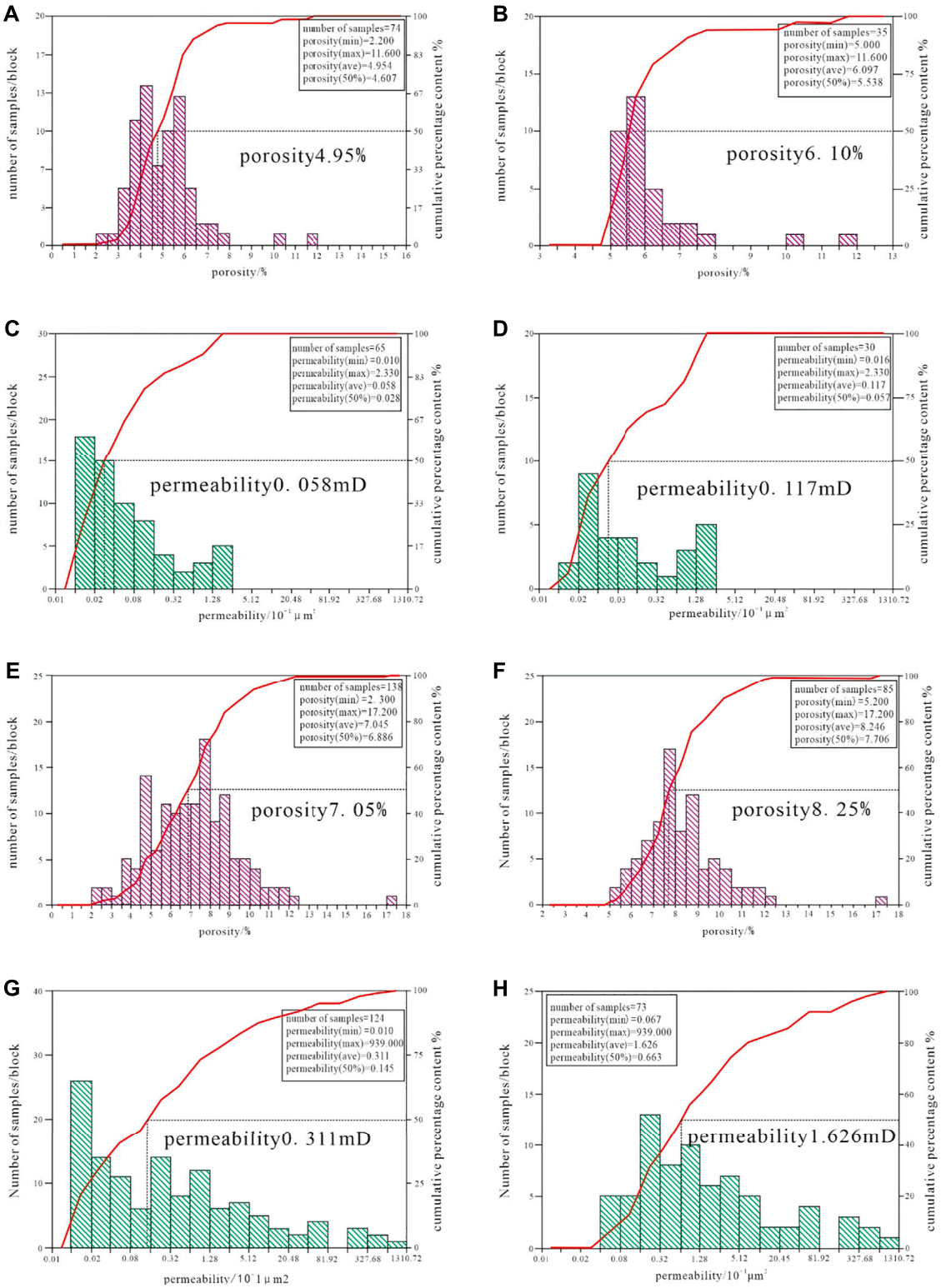

FIGURE 3
Porosity and permeability histograms of the Permian Upper Wuerhe Formation of Dinan 15 well block. **(A,B)** Porosity histogram of Section I, the Upper Wuerhe Formation; **(C,D)** Permeability histogram of Section I, the Upper Wuerhe Formation; **(E,F)** Porosity histogram of Section II, the Upper Wuerhe Formation; **(G,H)** Permeability histogram of Section II, the Upper Wuerhe Formation.

TABLE 2 Clay mineral content of the Upper Wuerhe Formation of Dinan 15 well block based on XDR.

Clay mineral content	Illite/smectite mixed layer	Illite	Kaolinite	Chloride	Sample qty
Range (%)	0–54.0	0–38.0	0–25.0	15.0–57.0	5
Average (%)	25.2	21.6	10.8	42.4	

TABLE 3 Statistical list of reservoir sensitivity analysis on the Upper Wuerhe Formation of Dinan 15 block.

No. of well	Depth of sample (m)	Experiment item	Porosity (%)	Kirschner permeability (mD)	Formation water permeability (mD)	Gas permeability (mD)	Damage rate (%)	Evaluation result
Dinan 081 well	4,022.77	Water sensitivity	4.88	0.517	0.0172	0.635	11.1	Weak
Dinan 10 well	3,398.52	Water sensitivity	4.27	0.282	0.0305	0.47	33.1	Below-middle
	3,398.52	Water and speed sensitivity	4.63	0.286	0.0314	0.474	10.5	Weak
	3,400	Water sensitivity	5.91	0.213	0.0269	0.403	33.8	Below-middle
	3,400	Water and speed sensitivity	6.31	0.285	0.0313	0.456	22.7	Weak
Dinan 12 well	3,447.57	Water and speed sensitivity	7.67	0.874	0.0634	1.58	19.4	Weak
	3,447.57	Water sensitivity	5.89	1.28	0.0268	2.47	45.2	Below-middle
Dinan 13 well	4,105.23	Water sensitivity	7.97	0.859	0.0428	1.54	47.2	Below-middle
	4,105.23	Water and speed sensitivity	8.85	2.75	0.138	3.34	47.9	Below-middle

below 5 $\mu m^2 \times 10^{-3}$ μm^2, and thus this section has poor physical characteristics and features typical super-low porosity and low permeability (Xiao et al., 2019; Zhang et al., 2020c; Zhang et al., 2022e; Yu et al., 2022). When compared with each other, Sections I and II of the Upper Wuerhe Formation are insignificantly different from each other in porosity, but the latter is better than the former regarding permeability.

3.3 Sensitivity characteristics

In order to identify the sensitivity characteristics of the Upper Wuerhe Formation glutenite reservoirs, this study conducted clay mineral X-ray diffraction (XRD) analysis on 5 core samples from the Upper Wuerhe Formation and experimental analysis on the reservoir characteristics of 9 samples in total from Dinan 081 well, 10 well, 12 well and 13 well of Dinan 15 well block. Since kaolinite, smectite, illite, chlorite, interstratified minerals, etc. have relatively large surface areas and extremely strong activities (like adsorbability, sensitivity to external fluid, etc.), they can significantly influence the injectability, adsorbability and modification of various injectants and are the main minerals that damage reservoirs. Therefore, the main factors that determine the degree of damage to the reservoir sensitivity are the content, constituent, distribution and attitude of clay minerals contained in clastic interstitial materials. The water sensitivity of a reservoir is the phenomenon where the reservoir permeability is decreased due to the expansion, dispersion, migration and blockage of clay minerals when incompatible external fluid enters the reservoir. The speed sensitivity of a reservoir means the possibility and degree of permeability decrease caused by migration and pore blockage of various particles in the reservoir due to the movement speed increase of fluid. According to the clay mineral XRD statistical results of the Upper Wuerhe Formation cores (Table 2), the primary clay mineral is chloride (15%–57%, average 42.4%), which actively reacts with acidic fluid, decreasing the physical characteristics of reservoirs, and thus is an acid sensitive mineral, and the secondary is illite-smectite mixed layers (0%–54%, average 25.2%), which are easily expanded with water and then block pores and thus are water sensitive minerals. Additionally, illite (0%–38%, average 21.6%) and kaolinite (0%–25%, average 10.8%) may migrate and block pores in the form of particles under the condition of high-speed fluid seepage, and thus are both speed sensitive minerals. Based on the

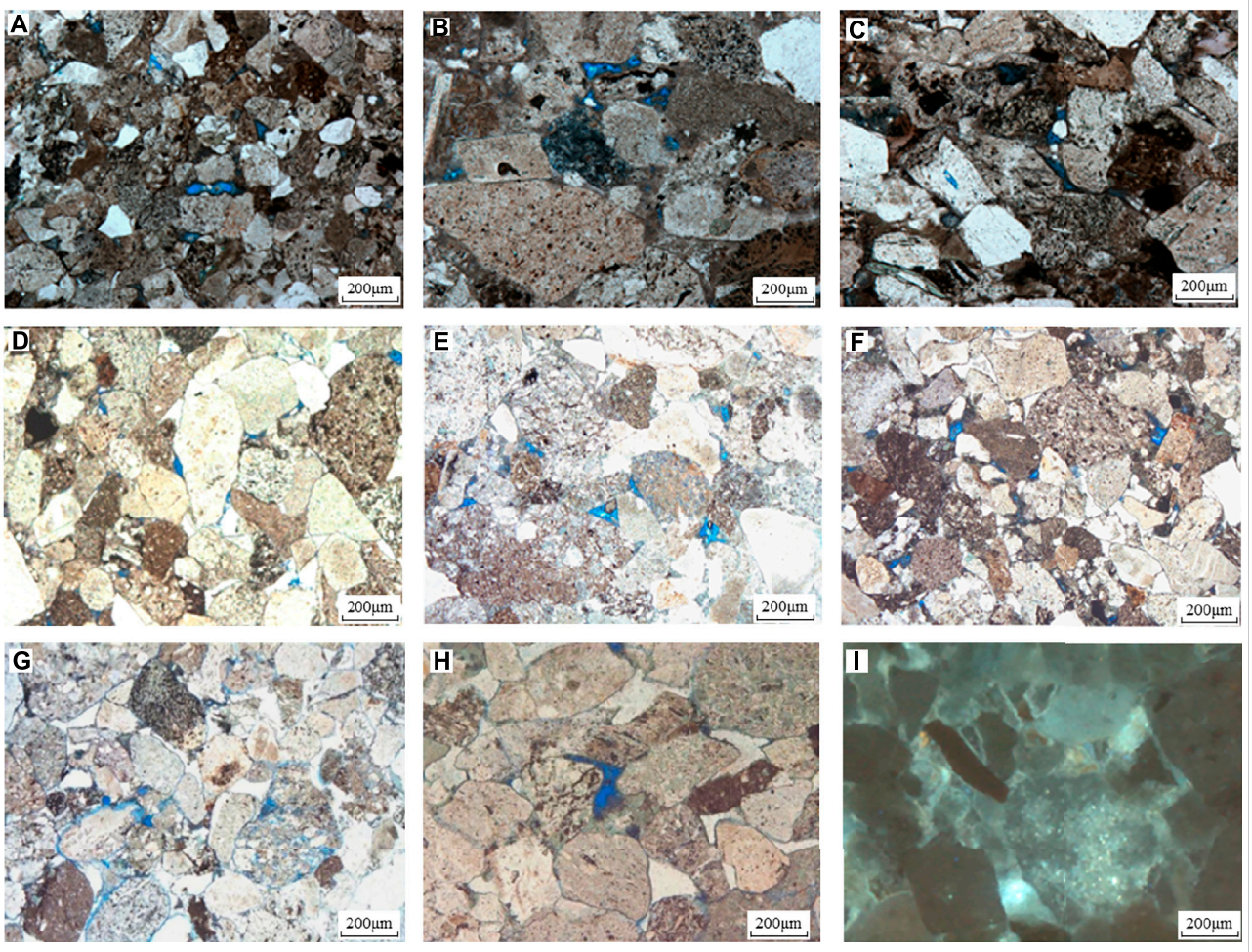

FIGURE 4
Microscopic thin section photos of pore types of the Permian Upper Wuerhe Formation reservoirs in the Dinan 15 well block. **(A)** Glutenite, intergranular pores 95%, intragranular dissolution pores 5%, Dinan 19 well, 3,926.8 m (P_3w_1); **(B)** Glutenite, intergranular pores 95%, intragranular dissolution pores 5%, Dinan 19 well, 3,922.57 m (P_3w_1); **(C)** Glutenite, intergranular pores 60%, intragranular dissolution pores 25%, tectonic fracture 15%, Dinan 19 well, 3,927.05 m (P_3w_1); **(D)** Medium sandstone, intergranular pores 95%, intragranular dissolution pores 4%, laumonite dissolution pores 1%, Dinan 14 well, 4,005.52 m (P_3w_1); **(E)** Sandy conglomerate, intergranular pores 60%, intragranular dissolution pores 30%, intergranular dissolution pores 10%, Dinan 15 well, 3,927.9 m(P_3w_2); **(F)** Sandy conglomerate, intergranular pores 70%, intergranular dissolution pores 20%, intragranular dissolution pores 10%, Dinan 15 well, 3,932.1 m (P_3w_2); **(G)** Sandy conglomerate, intergranular pores 50%, intergranular dissolution pores 20%, particle-edge fractures 20%, intragranular dissolution pores 10% Dinan 15 well, 3,728.87 m (P_3w_2); **(H)** pebbly unequal-particled sandstone, intergranular dissolution pores 90%, particle-edge fractures 5%, intragranular dissolution pores 5%, Dinan 8 well, 3,957.76m; **(I)** Pebbly unequal-particled lithic sandstone, part of the particles and interstitial materials luminous, Dinan 19 well, 3,924.99 m.

results of the experimental analysis on the reservoir sensitivity, it can be seen that the Upper Wuerhe Formation reservoirs feature below-middle water sensitivity and weak speed sensitivity (Table 3).

3.4 Reservoir space types and pore structures

Based on the cast thin section and SEM data combined with the pore characteristics, it is believed that the reservoir space types of the Upper Wuerhe Formation reservoirs of Dinan 15 well in the study area are diverse and dominated by intergranular pores, followed by intergranular dissolution pores, intragranular dissolution pores, and micro-fractures (Figure 4). Intergranular pores, which are mainly developed in glutenite and sandy conglomerate, are the preserved primary pores that have not been damaged by diagenesis; dissolution pores are divided into inter- and intra-granular ones and they are mainly developed in medium sandstone and gravel-bearing inequigranular sandstones. They are the secondary pores produced by the interaction between dissolution fluid and surrounding rock. Micro-fractures are also common in the

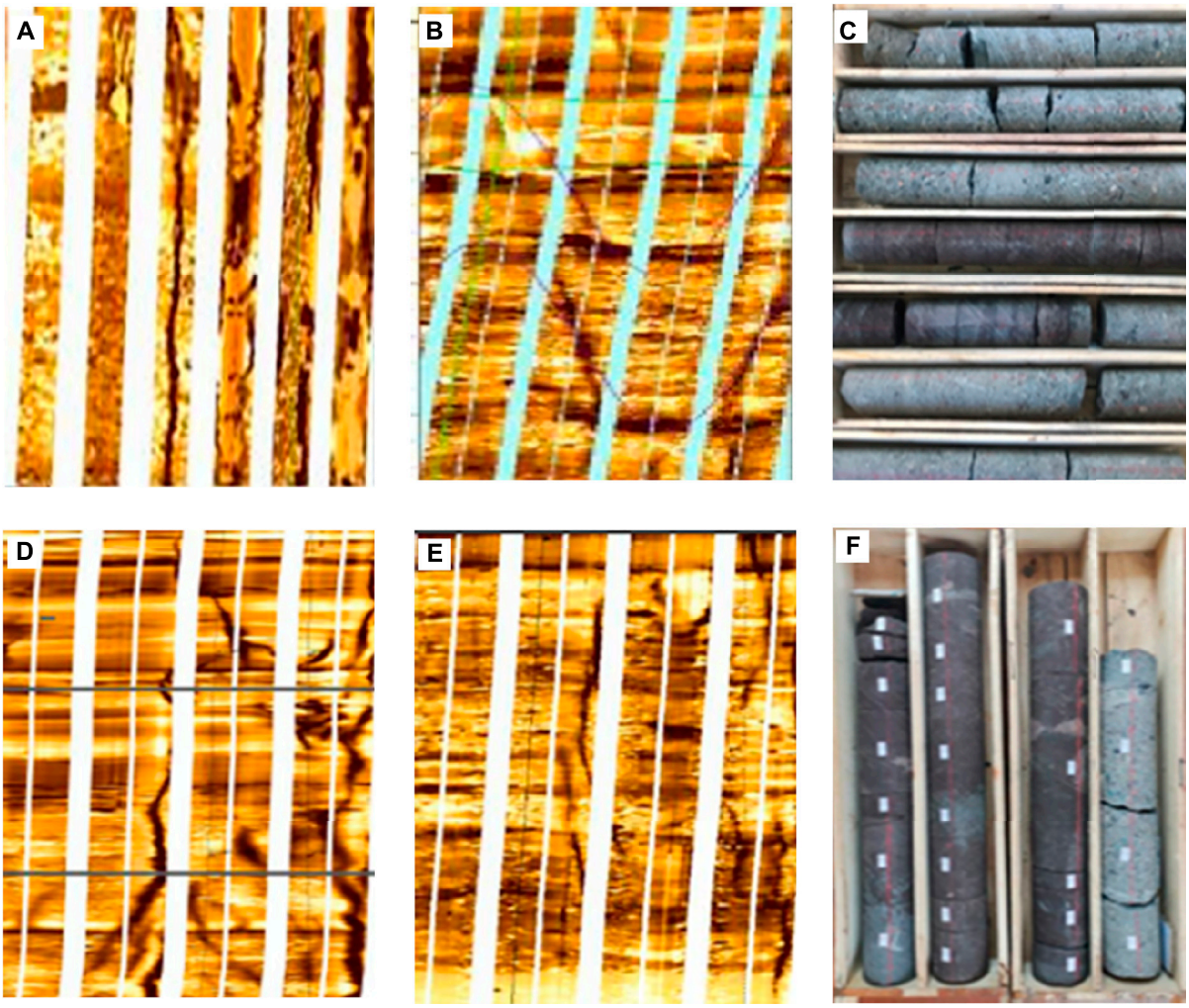

FIGURE 5
Development characteristics of fractures in imaging resistivity and cores. **(A)**. Glutenite, Dinan 14 well, 4000 m–4008 m; **(B)** Glutenite, Dinan 15 well, 3721 m–3735 m; **(C)** Core, Dinan 15 well, 3,731.8 m–3,739.1 m; **(D)** Glutenite, Dinan 14 well, 4,000 m–4,008 m; **(E)** Glutenite, Dinan 15 well, 3,795 m–3,797 m; **(F)** Core, Dinan 15 well, 3,796.5 m–3,799.8 m.

glutenite reservoirs in the study area. Due to the high content of brittle particles such as quartz and feldspar in the glutenite, a series of fractures are generated along the grain edges under the action of stress, providing space for oil and gas migration and storage.

According to the data of core collection and FMI micro-resistivity imaging, vertical fractures and high angle fractures exist in the Upper Wuerhe Formation reservoirs and are dominated by micro-factures (Figure 5). The internal edges of some fractures are straight, with a high degree of opening, and appear in groups. It is believed that the stress field changes brought about by regional tectonic activities form structural fractures that have a low filling degree and most of them can become effective seepage channels (Figures 5A,B); some fractures are not straight and have low degree of opening. Although the extension direction is consistent but the length is different, the interior is mostly filled with secondary minerals or organic matter, and the contribution to the reservoir and permeability is limited (Figures 5D, E)

10 samples, collected from Sections I and II of the Upper Wuerhe Formation of Dinan 15 well, were selected for high-pressure mercury injection experiment (Figure 6). Based on the experiment results, it can be seen that the mercury injection curves of the Upper Wuerhe Formation take on a shape of slope, indicating that the reservoirs feature slightly fine skewness, poor sorting, small pores and fine throat. The maximum capillary radius of the reservoirs is 0.817–32.978μm, with the average of 11.687μm, and their displacement pressure is 0.0223–0.9MPa, with the average of 0.501 MPa. This indicates that the glutenite reservoir in the studied section has a better pore-throat ratio and has a certain seepage capacity.

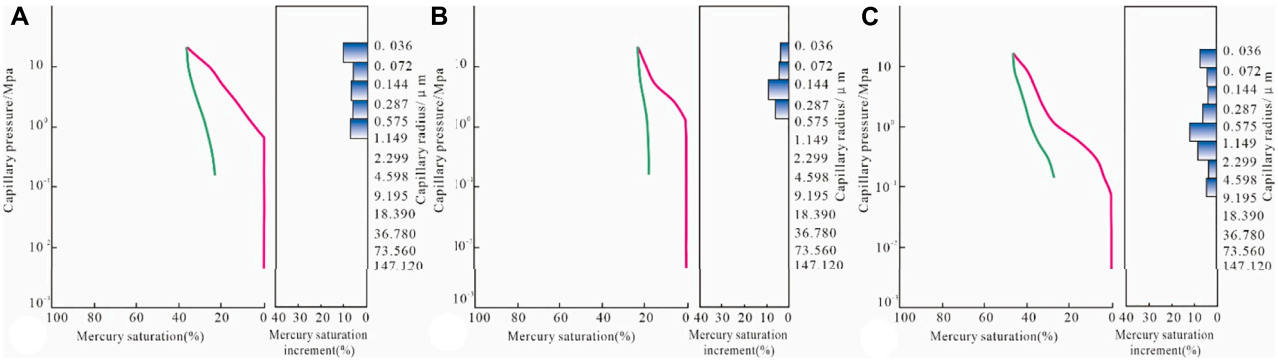

FIGURE 6
Capillary pressure curve of the Permian Upper Wuerhe reservoirs of Dinan 15 well block. **(A,B)** Capillary pressure curve of Section I reservoirs of the Upper Wuerhe Formation; **(C)** Capillary pressure curve of Section II reservoirs of the Upper Wuerhe Formation.

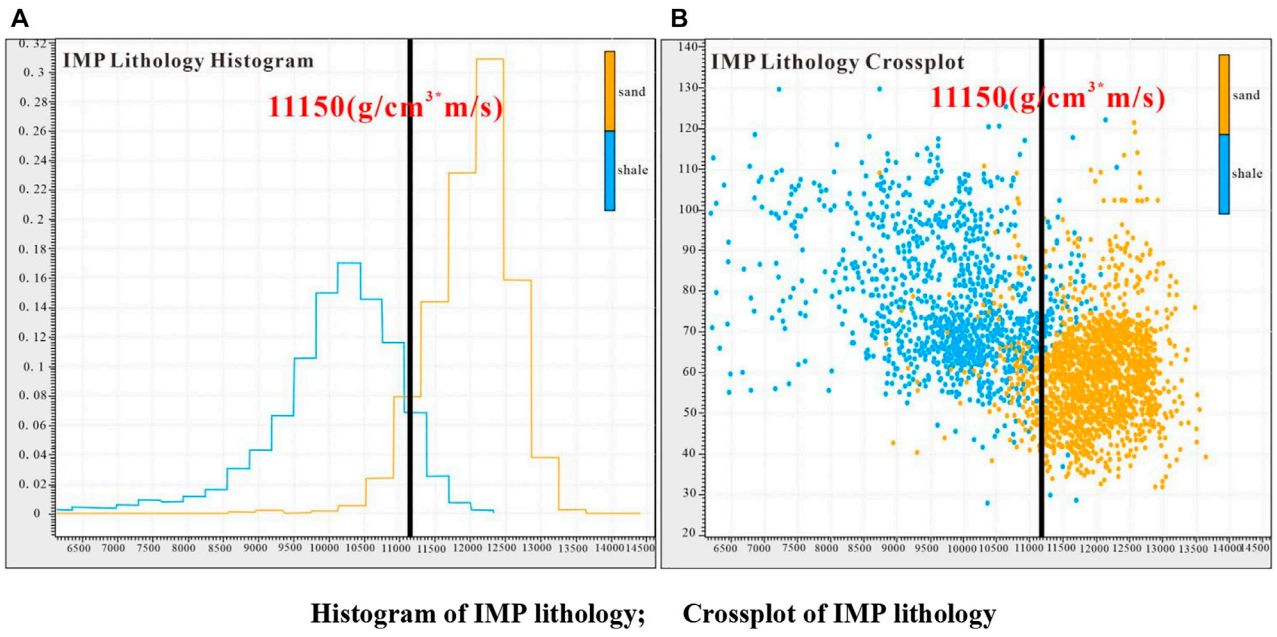

FIGURE 7
Gama-wave impedance crossplot of the Upper Wuerhe Formation of the Dinan 15 well block. **(A)** Histogram of IMP lithology; **(B)** Crossplot of IMP lithology.

3.5 Log response characteristics of reservoirs

The rock types of the Permian Upper Wuerhe Formation reservoirs of the Dinan 15 well block include glutenite, pebbly sandstone, medium–fine sandstone, siltstone, argillaceous siltstone and silty mudstone. The parameters, including sound waves, density, gamma, resistivity, wave impedance, etc. of the target sections of all prospecting wells and evaluation wells in the selected well block were adopted for analysis on the reservoir sensitivity parameters. According to the logging results and log interpretation combined with lithology and the analysis on the characteristics of the longitudinal wave impedance corresponding to the reservoirs, the lithology corresponding to the high-impedance-value part of the Permian Upper Wuerhe Formation of the Dinan 15 well block is glutenite and sandstone, with the average > 11,150 mg/scm, while that corresponding to the low-impedance-value part is mudstone, with a wave impedance value <10,000 mg/scm generally (Figures 7, 8).

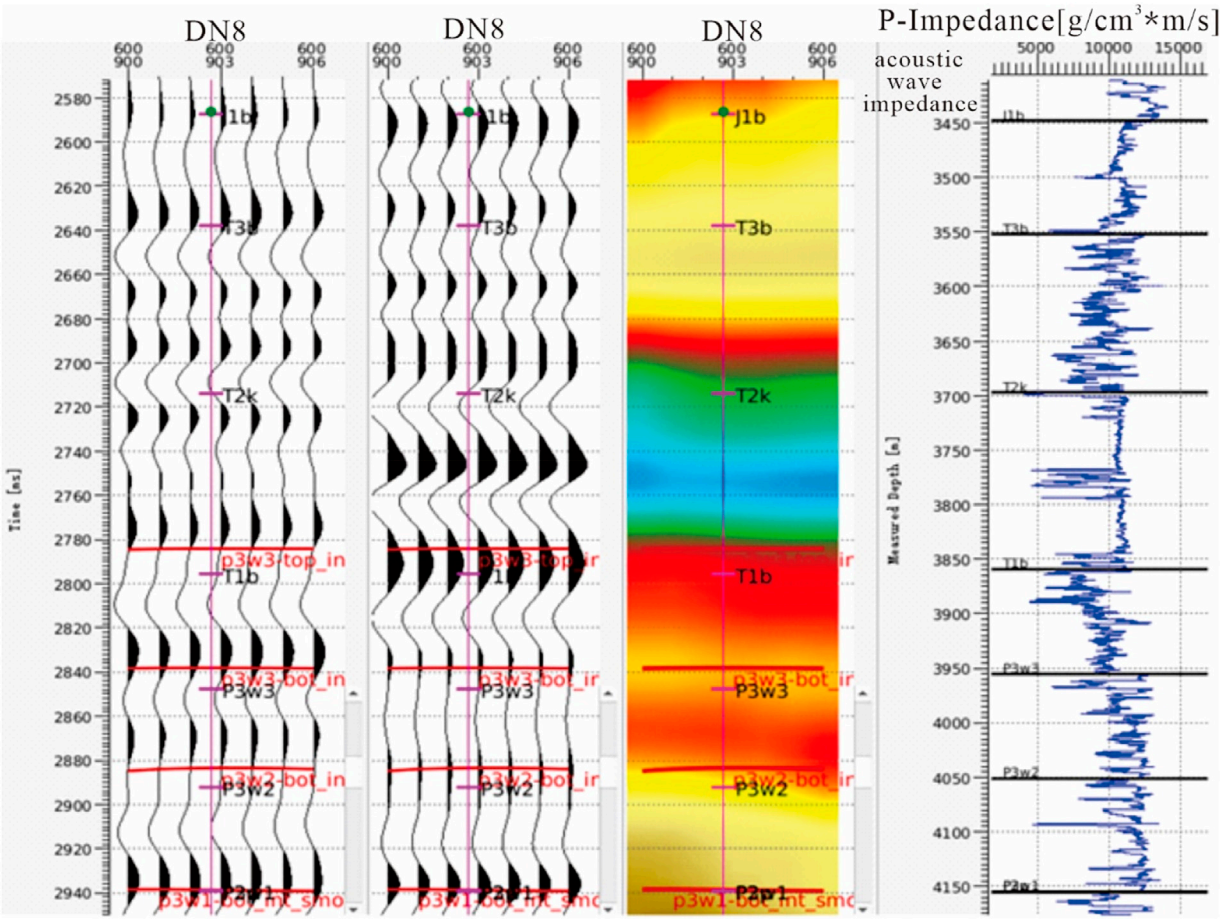

FIGURE 8
Identification results of reservoir rock types based on wave impedance parameters–a case of Dinan 8 well.

4 Reservoir prediction

4.1 Criteria for reservoir evaluation

Lithology reflects the material basis of a reservoir, physical characteristics embody the basic reserve capacity, sensitivity represents the anti-damage capability of a reservoir, and pore structures indicate the micro distribution regularities of reservoir space. Therefore, based on the above research and analysis, with lithology, physical characteristics, sensitivity, reservoir space types and microstructure characteristics adopted as the key parameters, the criteria for reservoir evaluation were established for the tight reservoirs in the study area, which are classified into three types of reservoirs, i.e., Type I, Type II, and Type III, with the reservoir quality decreasing from Type I to Type III (Table 4).

Type I reservoirs: the lithology is dominated by glutenite and pebbly sandstone. The average porosity and permeability are higher than 12% and 5 $\mu m^2 \times 10^{-3}$ μm^2, respectively. The reservoirs are weak water-sensitive and weak speed-sensitive. The primary reservoir space is intergranular pores and laumonite dissolution pores, and the secondary is intragranular dissolution pores. The pore throats are dominated by fine skewness, and are a combination of macro-mesopores and fine pore throats, with good pore throat connectivity. The maximum connecting pore throat radius is 9.195 μm–32.978 μm, and the log response is high impedance response.

Type II reservoirs: the lithology is dominated by medium–fine sandstone and siltstone. The average porosity and permeability are between 8% and 12% and 2.56 μm^2 $\times 10^{-3}$ μm^2~5 $\times$ $10^{-3}\mu m^2$, respectively. The reservoirs are below-middle water-sensitive and below-middle speed-sensitive. The primary reservoir space is intergranular pores and laumonite dissolution pores, and the secondary is intragranular dissolution pores. The pore throats are dominated by fine skewness, and are a combination of small-micropores and fine pore throats, with good pore throat connectivity. The maximum connecting pore throat radius is 1.267 μm–9.195 μm, and the log response is high impedance–medium impedance response.

TABLE 4 Criteria for reservoir classification established based on lithology, physical characteristics, sensitivity, reservoir space types, and microstructure characteristics.

Reservoir type	Lithology	Physical characteristics		Sensitivity	Reservoir space type	Pore structure characteristics		Log response
		Porosity/%	Permeability/$\times10^{-3}\mu m^2$			Pore throat distribution	Pore size distribution/μm	
I	Glutenite Pebbly sandstone	> 12	> 5	Weak water-sensitive Weak speed-sensitive	Primary: intergranular pores, laumonite dissolution pores Secondary: intragranular dissolution pores	Fine skewness Macro-mesopores Fine throat	9.195~32.978 17.719	High impedance
II	Middle–fine sandstone Siltstone	8–12	2.56–5	Below-middle water-sensitive Below-middle speed-sensitive	Primary: intergranular pores, laumonite dissolution pores Secondary: intragranular dissolution pores	Fine skewness Small-micropores Fine throat	1.267~9.195 5.442	Medium impedance–high impedance
III	Argillaceous siltstone Silty mudstone	< 8	< 2.56	Above-middle water-sensitive Above-middle speed-sensitive	Combination of a few residual intergranular pores and the internal micropores of interstitial materials	Fine skewness Small-micropores Micro throat	0.036~1.267 0.3195	Medium impedance–low impedance

Type III reservoirs: the lithology is dominated by argillaceous siltstone and silty mudstone. The average porosity and permeability are lower than 8% and 2.56 $\mu m^2 \times 10^{-3}\mu m^2$, respectively. The reservoirs are above-middle water-sensitive and above-middle speed-sensitive. The primary reservoir space is a combination of a few residual intergranular pores and the internal micropores of interstitial materials. The pore throat distribution is dominated by fine skewness and is a combination of small-micropores and micro pore throats, with poor pore throat connectivity. The maximum connecting pore throat radius is 0.036 μm–1.267 μm, and the log response is medium impedance–low impedance response.

4.2 Reservoir prediction

4.2.1 Lateral reservoir prediction

Based on the reservoir evaluation criteria established above combined with the indication of single well oil-bearing characteristics, Dinan 8 well, Dinan 083 well, Dinan 15 well, Dinan 12 well and Dinan 121 well in the west of the study area were selected to establish a well-tie profile in order to characterize the lateral reservoir distribution rules. As shown in Figure 9, Type I reservoirs pass through Dinan 083 and 15 wells along the direction from southwest to northeast, and are mainly distributed in the top and middle parts of Dinan 083 and 15 wells. Their single layers are thin and feature sand-mud interbedding, with continuously sedimentary sand bodies, good physical characteristics and oil-bearing characteristics. Oil and gas are in the same layer and the current production of oil and gas is 339.11t/d and 27980m^3/d, respectively. Besides, Type II reservoirs pass through Dinan 8, 083 and 15 wells along the direction from southwest to northeast, and are mainly distributed in the top and bottom parts of Dinan 8 well, and the bottom parts of Dinan 083 and 15 wells. Their single layers are relatively thick and feature local continuation, with good physical characteristics and oil-bearing characteristics. Oil-water and oil-gas are in the same layer and the current production of oil and gas of Dinan 8 and 083 wells is 26.37 t/d and 2,610 m^3/d, and 83.59 t/d and 13,190 m^3/d, respectively, and the oil production of Dinan 15 well is 42.02 t/d. Last but not least, Type III reservoirs pass through

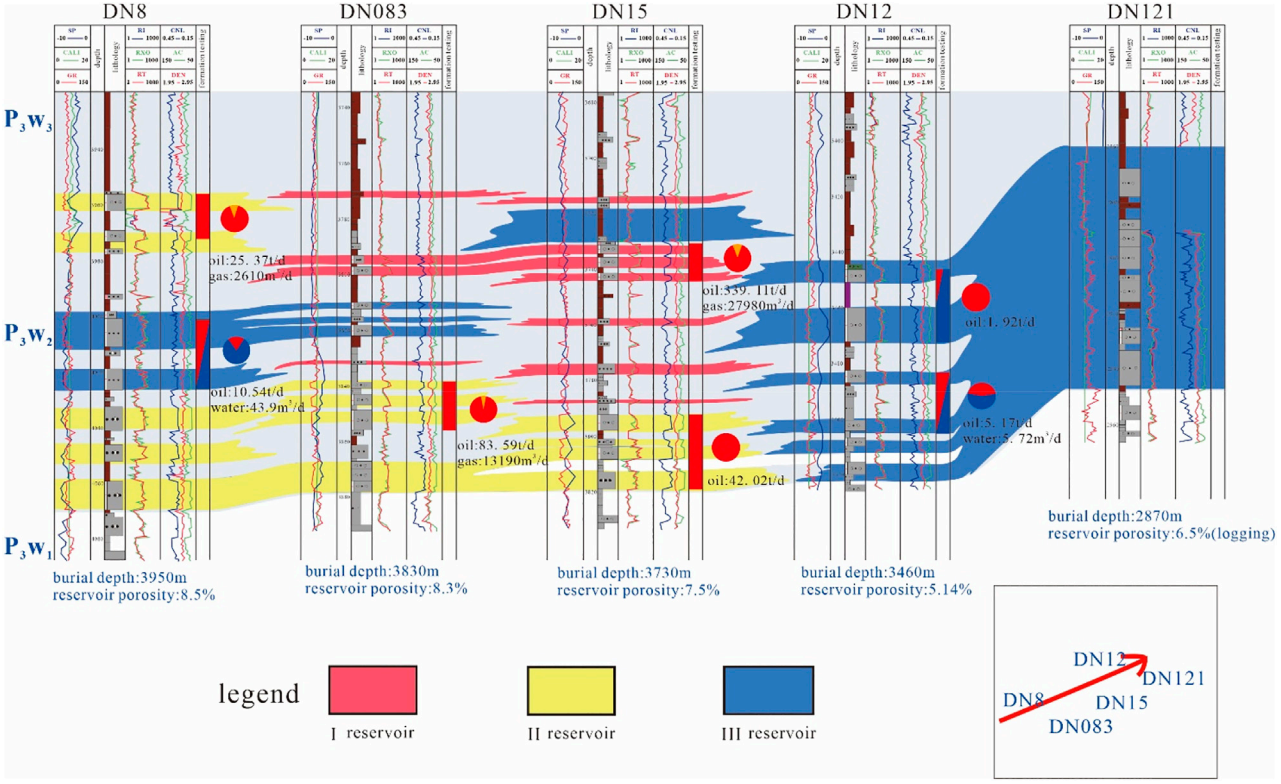

FIGURE 9
Prediction on reservoir distribution on the Dinan 8 well–Dinan 15 well–Dinan 121 well profile.

Dinan 8, 083, 15, 12 and 121 wells along the direction from southwest to northeast, and are mainly distributed in Dinan 121 well, the middle and bottom parts of Dinan 12 well, and the middle part of Dinan 8 well, and partially in the top part of Dinan 15 well and the middle part of Dinan 083 well along the direction from southwest to northeast. Their single layers are thick and feature block structures, with relatively poor physical characteristics and oil-bearing characteristics. The oil-bearing layers and oil-water are in the same layer and the current production of oil and gas of Dinan 8 and 12 wells is 10.54 t/d and 43.9 m^3/d, and 7.09 t/d and 5.72 m^3/d, respectively.

4.2.2 Reservoir plane prediction

Based on the criteria for reservoir evaluation and the prediction results of single-well and well-tie reservoirs, the diagrams of reservoir plane distribution were drawn. Wave impedance was utilized to distinguish reservoir areas and non-reservoir areas (Figures 10A,B). The grey-black areas are the low values of wave impedance, representing the non-reservoir areas, while the red-yellow areas are the high values of wave impedance, representing the reservoir areas. Plane prediction was conducted on the different reservoir types of P_3w_1 and P_3w_2 based on the plane distribution characteristics, including the parameters of lithology, physical characteristics, sensitivity, pore structures, etc., in accordance with the reservoir classification criteria (Figures 10C,D).

According to the plane distribution diagram of P_3w_1 reservoirs, Type I reservoirs are mainly distributed in the west of the study area, specifically in the areas of Dinan 20, 18, 21, 13, 10, 8, and 081 wells, with an area around 314 km^2. Besides, Type II reservoirs are mainly distributed in the center of the study area, specifically in the areas of Dinan 12, 086, 15, 083, 084, 19 085 and 089 wells, with an area around 529.87 km^2. Last but not the least, Type III reservoirs are mainly distributed in the east of the study area, specifically in the areas of Dinan 1, 2, 3, 201, 142 and 17 wells, with an area around 156.8 km^2.

According to the plane distribution diagram of P_3w_2 reservoirs, Type I reservoirs are mainly distributed in the west and east of the study area, specifically in the areas of Dinan 20, 201, 142, 13, 084, 083, 8, 081 and 141 wells, with an area around 530.66 km^2. Besides, Type II reservoirs are mainly distributed in the center and west of the study area, specifically in the areas of Dinan 21, 18, 3, 1, 2, 088, 12, 086, 15, 085, 14, 089 and 17 wells, with an area around 961.63 km^2. Last but not least, Type III reservoirs are mainly distributed in the southeast of the study

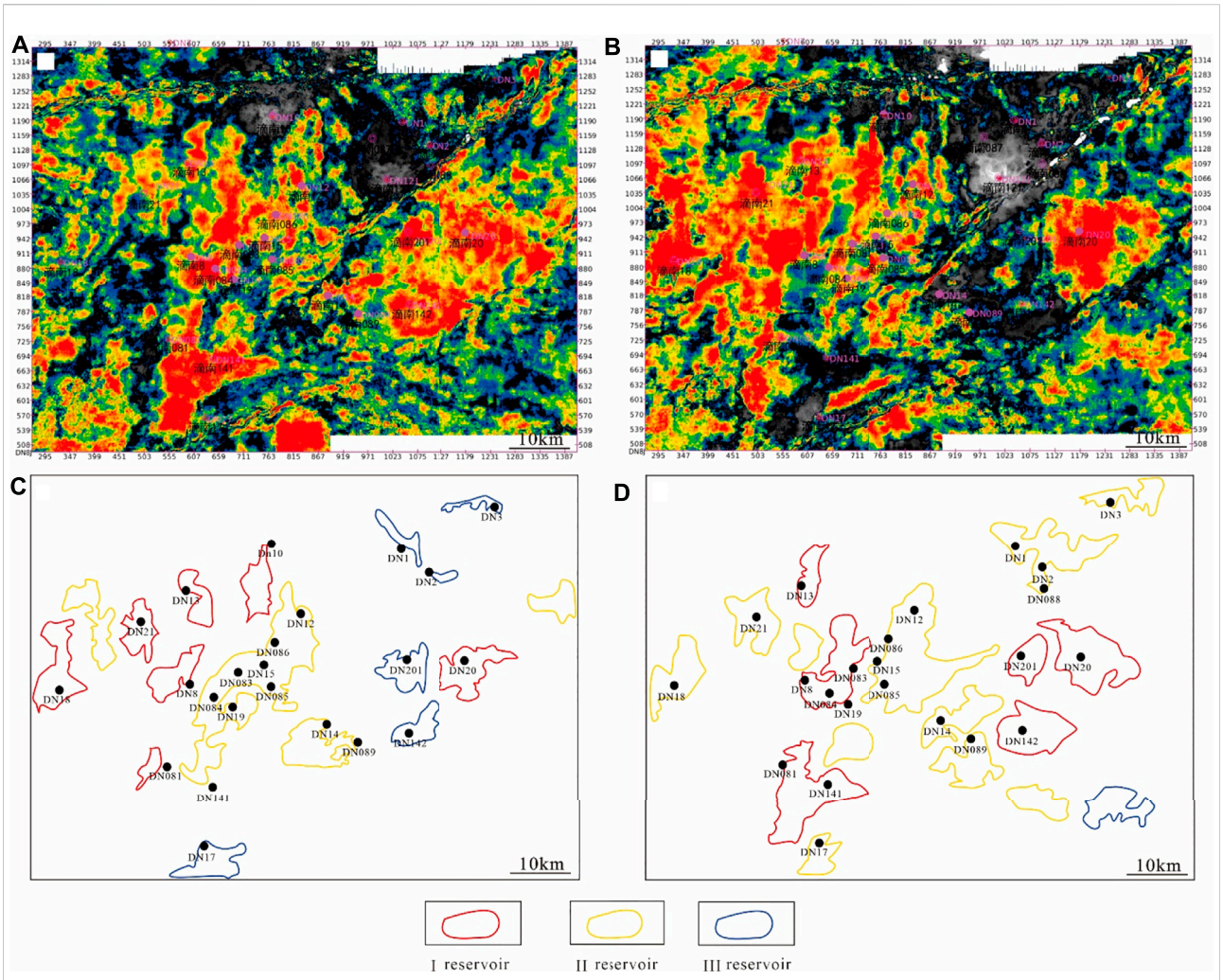

FIGURE 10
Inversion plans of the Permian Upper Wuerhe Formation of the Dinan 15 well block and plane prediction diagrams of Type I, II and III reservoirs. **(A)** Inversion plan of Section I, the Permian Upper Wuerhe Formation of the Dinan 15 well block; **(B)** Inversion plan of Section II, the Permian Upper Wuerhe Formation of the Dinan 15 well block; **(C)** Plane distribution diagram of Types I, II and III reservoirs of Section I, the Permian Upper Wuerhe Formation of the Dinan 15 well block; **(D)** Plane distribution diagram of Types I, II and III reservoirs of Section II, the Permian Upper Wuerhe Formation of the Dinan 15 well block.

area, specifically close to the areas of Dinan 142 and 20 wells, with an area of around 78.5 km^2.

5 Conclusion

(1) The lithology of the Upper Wuerhe Formation in the Dinan 15 well area is dominated by gray glutenite; at the same time, various rock types such as glutenite and medium sandstone are developed;

(2) The glutenite reservoirs of the Upper Wuerhe Formation in the Dinan 15 well block is an ultra-low porosity and ultra-low permeability reservoir, with moderately weak water sensitivity and weak velocity sensitivity. The shape of the mercury intrusion curve and the pore throat radius distribution of the samples show that the reservoir is skewed, poorly sorted, and has the characteristics of small pores and thin throats.

(3) This work constructed evaluation criteria for reservoirs from I to III by utilizing lithology, physical properties, sensitivity, reservoir space type, and microstructural characteristics as key parameters. The favorable reservoir distribution area is mainly located in the west of the block, which is the focus of the next exploration of the Upper Wuerhe Formation area.

Data availability statement

The raw data supporting the conclusions of this article will be made available by the authors, without undue reservation.

Author contributions

WX contributed to conception and design of the study. SX organized the database. YX performed the statistical analysis. WX wrote the first draft of the manuscript. SX, YX, and YY wrote sections of the manuscript. All authors contributed to manuscript revision, read, and approved the submitted version.

Funding

This study was supported by the open funds from the National Natural Science Foundation of China (No. 42102192), the open experiment fund of Southwest Petroleum University (2021KSP02029), and the Science and Technology Cooperation Project of the CNPC-SWPU Innovation Alliance. We sincerely appreciate all reviewers and the handling editor for their critical comments and constructive suggestions.

Conflict of interest

The authors declare that the research was conducted in the absence of any commercial or financial relationships that could be construed as a potential conflict of interest.

Publisher's note

All claims expressed in this article are solely those of the authors and do not necessarily represent those of their affiliated organizations, or those of the publisher, the editors and the reviewers. Any product that may be evaluated in this article, or claim that may be made by its manufacturer, is not guaranteed or endorsed by the publisher.

References

Bian, H., Han, B., Wang, F., Liu, G., Li, X., and Guo, Z. (2020). Characteristics and classification of glutenite reservoirs in Niudong area, north margin of Qaidam Basin. *J. Xi'an Univ. Sci. Technol.* 40 (5), 894–901. doi:10.13800/j.cnki.xakjdxxb.2020.0519

Cai, Y., Xia, Y., Huang, X., Wang, X., and Li, Y. (2019). Application of multi-attribute fusion technique in sedimentary facies research. *Collect. Works 2019 Geophys. Explor. Technol. Seminar China Petroleum Soc.* 2019, 723–726.

Ding, X. (2016). Analysis of hydrocarbon Genesis and accumulation stage of Dongdaohaizi Sag in Junggar Basin. *Sci. Technol. Eng.* 16 (10), 80–84+88.

Du, J., Zhi, D., Tang, Y., Jia, C., Yang, X., Abulimity, Y., et al. (2019). Prospects in upper permian and strategic discovery in shawan sag, Junggar Basin. *China Pet. Explor.* 24 (01), 24–35. doi:10.3969/j.issn.1672-7703.2019.01.004

Feng, T. (2017). *Permian tectonic-stratigraphic sequence and basin evolution in Junggar Basin*. Beijing: China University of Geosciences.

Fu, S., Lei, P., Xu, X., Cao, Y., Liu, Z., Zhang, S., et al. (2019). The characteristics and their controlling factors on reservoir in permian lower urho Formation in Mahu sag, Junggar Basin. *Nat. Gas. Geosci.* 30 (04), 468–477. doi:10.11764/j.issn.1672-1926.2019.01.015

Gao, F. (2021). Influence of hydraulic fracturing of strong roof on mining-induced stress insight from numerical simulation. *J. Min. Strata Control Eng.* 3 (2), 023032. doi:10.13532/j.jmsce.cn10-1638/td.20210329.001

Guan, X., Pan, S., Qu, Y., Xu, D., Zhang, H., Ma, Y., et al. (2021). Discovery and hydrocarbon exploration potential of beach-bar sand in Shawan Sag, Junggar Basin. *Lithol. Reserv.* 33 (01), 90–98. doi:10.10108/yxyqc.2021109

Hu, X., Qu, Y., Hu, S., Pan, J., Lu, Y., Xu, D., et al. (2020). Geological conditions and exploration potential of shallow oil and gas in slope area of Mahu Sag, Junggar Basin. *Lithol. Reserv.* 32 (02), 67–77. doi:10.12108/yxyqc.20200207

Hu, X., Ding, X., Zhang, X., Lei, L., Wang, X., et al. (2021a). Glutenite reservoir characteristics and main controlling factors of Es_3-Es_4 in northern zone of Bonan. *J. Northeast Petroleum Univ.* 45 (01), 55–61. doi:10.3969/j.issn.2095-4107.2021.01.006

Hu, X., Zou, H., Hu, Z., Li, Y., Huang, Y., Fu, X., et al. (2021b). Reservoir characteristics and main controlling factors of glutenite reservoir in fan dalta glutenite:a case study of the Upper Urho Formation of Permian in the east slope of Dongdaohaizi Sag, Junggar Basin. *J. Northeast Petroleum Univ.* 45 (06), 15–26. doi:10.3969/j.issn.2095-4107.2021.06.002

Huang, H. X., Li, R. X., Jiang, Z. X., Li, J., Chen, L., et al. (2020). Investigation of variation in shale gas adsorption capacity with burial depth: Insights from the adsorption potential theory. *J. Nat. Gas. Sci. Eng.* 73, 103043. doi:10.1016/j.jngse.2019.103043

Jin, G., Wang, T., Liu, Z., Xie, R., Shao, L., and Li, B. (2022). Classification and productivity prediction of glutenite reservoirs based on NMR logging. *ACTA PET. SIN.* 43 (5). doi:10.7623/syxb202205006

Jin, J., Luo, X., Liao, J., Yu, Q., Wang, D., Zhao, W., et al. (2015). Geochemical characteristics of permian Pingdiquan Formation hydrocarbon source rocks in Dongdaohaizi sag, Junggar Basin, China. *J. Chengdu Univ. Technol. Sci. Technol. Ed.* 42 (02), 196–202. doi:10.3969/j.issn.1671-9727.2015.02.07

Jin, J., Xun, K., Hu, W., Xiang, B., Wang, J., Cao, J., et al. (2017). Diagenesis of its influence on coarse clastic reservoirs in the Baikouquan Formation of Western slope of the Mahu depression, Junggar Basin. *Oil Gas Geol.* 38 (02), 323–333+406. doi:10.11743/ogg20170212

Kang, H., Xu, G., Wang, B., Wu, Y., Jiang, P., Pan, J., et al. (2019). Forty years development and prospects of underground coal mining and strata control technologies in China. *J. Min. Strata Control Eng.* 1 (1), 013501. doi:10.13532/j.jmsce.cn10-1638/td.2019.02.002

Kuang, L., Tang, Y., Lei, D., Wu, T., and Qu, J. (2014). Exploration of fan-controlled large-area lithologic oil reservoirs of triassic Baikouquan Formation in slope zone of Mahu depression in Junggar Basin. *China Pet. Explor.* 19 (06), 14–23. doi:10.13532/j.jmsce.cn10-1638/td.2019.02.002

Li, H. (2022). Research progress on evaluation methods and factors influencing shale brittleness: A review. *Energy Rep.* 8, 4344–4358. doi:10.1016/j.egyr.2022.03.120

Li, H., Qin, Q., Zhang, B., Ge, X., Hu, X., Fan, C., et al. (2020). Tectonic fracture Formation and distribution in ultradeep marine carbonate gas reservoirs: A case study of the maokou Formation in the jiulongshan gas field, sichuan basin, southwest China. *Energy fuels* 34 (11), 14132–14146. doi:10.1021/acs.energyfuels.0c03327

Li, H., Tang, H., Qin, Q., Zhou, J., Qin, Z., Fan, C., et al. (2019). Characteristics, formation periods and genetic mechanisms of tectonic fractures in the tight gas sandstones reservoir: A case study of xujiahe Formation in YB area, sichuan basin, China. *J. Petroleum Sci. Eng.* 178, 723–735. doi:10.1016/j.petrol.2019.04.007

Li, Y. Y., Qian, G., Gao, Y., Qin, J., Huang, W., Lu, S., et al. (2018). Identification criterion of the geological "sweet point" of conglomerate tight reservoir and its application of Baikouquan formation in Mahu sag, Junggar basin. *J. Northeast Petroleum Univ.* 42 (06), 85–94+10. doi:10.3969/j.issn.2095-4107.2018.06.009

Lin, H., Liu, P., Wang, T., Chen, S., Mu, X., Liu, Y., et al. (2019). Diagenetic evolution mechanism of deep glutenite reservoirs based on differences in parent rock types: A case study of lower submember of member 3 of shahejie Formation in chezhen sag, Bohai Bay Basin. *Acta Pet. Sin.* 40 (10), 1180–1191. doi:10.7623/syxb201910004

Liu, M. (2015). *Genesis analysis of low porosity and low permeability reservoirs in the Upper Wuerhe Formation of the Fifth Block*. Wuhan: Yangtze University.

Liu, M., Xie, R., Guo, J., and Jin, G. (2018). Characterization of pore structures of tight sandstone reservoirs by multifractal analysis of the NMR T2 distribution. *Energy fuels.* 32 (12), 12218–12230. doi:10.1021/acs.energyfuels.8b02869

Lu, H., Luo, H., Luo, F., Mao and Dengzhou (2021). Fan controlled large-area accumulation conditions and mode of upper Wuerhe Formation in MH1 well zone of Mahu sag. *Special Oil Gas Reservoirs* 28 (01), 42–50. doi:10.3969/j.issn.1006-6535.2021.01.006

Pang, X., Niu, C., Du, X., Wang, Q., and Dai, L. (2020). Quantitative characterization of differences in glutenite reservoir in the Member 1 and 2 of Shahejie Formation in the northeastern margin of Shijiutuo uplift, Bohai Sea. *Acta Pet. Sin.* 41 (9), 1073–1088. doi:10.7623/syxb202009004

Qu, J., Zhang, L., Wu, J., and You, X. (2017). Characteristics of sandy conglomerate reservoirs and controlling factors on physical properties of Baikouquan Formation in the Western slope of Mahu sag, Junggar Basin. *Xinjiang Pet. Geol.* 38 (1), 1–6. doi:10.7657/XJPG20170101

Wang, J., Zhang, C., Zheng, D., Song, W., and Ji, X. (2020b). Stability analysis of roof in goaf considering time effect. *J. Min. Strata Control Eng.* 2 (1), 013011. doi:10.13532/j.jmsce.cn10-1638/td.2020.01.005

Wang, R., Zheng, M., Yang, S., Zhao, X., Jiang, Y., Wan, M., et al. (2022). Characteristics and controlling factors of weakly cemented glutenite reservoir in permian upper urho formation, south slope of Mahu sag. *Special Oil Gas Reservoirs* 29 (01), 23–30. doi:10.3969/j.issn.1006-6535.2022.01.004

Wang, Y., Cui, M., Liu, L., and Dan, L. (2020a). Pore throat characteristics of glutenite reservoirs in Cretaceous of Fangzheng Depression. *J. Northeast Petroleum Univ.* 44 (02), 36–45. doi:10.3969/j.issn.2095-4107.2020.02.004

Xiao, J., Hao, Q., Zhang, S., and Fan, S. (2020). Influence of oil well casing on the law of strata pressure in working face. *J. Min. Strata Control Eng.* 2 (1), 013522. doi:10.13532/j.jmsce.cn10-1638/td.2020.01.003

Xiao, M., Yuan, X., Wu, S., Cao, Z., Tang, Y., Xie, Z., et al. (2019). Conglomerate reservoir characteristics of and main controlling factors for the Baikouquan Formation, Mahu sag, Junggar Basin. *Earth Sci. Front.* 26 (01), 212–224. doi:10.13745/j.esf.sf.2018.12.7

Xu, L., Chang, Q., Tao, Q., and Wang, W. (2017). Reservoir characteristics and control factors of Baikouquan Formation in triassic, mabei oilfield, Junggar Basin. *Geol. Rev.* 63 (S1), 277–278. doi:10.16509/j.georeview.2017.s1.132

Yang, B., Zhang, Z., and Zhang, C. (2020). Investigation of reservoir classification of glutenites in Bozhong 19-6 gas field. *Contemp. Chem. Ind.* 49 (12), 2786–2790. doi:10.13840/j.cnki.cn21-1457/tq.2020.12.033

Yu, X., Bian, J., and Liu, C. (2022). Determination of energy release parameters of hydraulic fracturing roof near goaf based on surrounding rock control of dynamic pressure roadway. *J. Min. Strata Control Eng.* 4 (1), 013016. doi:10.13532/j.jmsce.cn10-1638/td.20210908.001

Zhang, H. (2014). *Key sources of oil and gas reservoirs and accumulation in the northern belt of the haizi depression in the east of the Junggar Basin*. Chengdu: Southwest Petroleum University.

Zhang, K., Jia, C., Song, Y., Jiang, S., Jiang, Z., Wen, M., et al. (2020a). Analysis of lower cambrian shale gas composition, source and accumulation pattern in different tectonic backgrounds: A case study of weiyuan block in the upper yangtze region and xiuwu basin in the lower yangtze region. *Fuel* 263 (2020), 115978. doi:10.1016/j.fuel.2019.115978

Zhang, K., Jiang, S., Zhao, R., Wang, P., Jia, C., and Song, Y. (2022a). Connectivity of organic matter pores in the Lower Silurian Longmaxi Formation shale, Sichuan Basin, Southern China: Analyses from helium ion microscope and focused ion beam scanning electron microscope. *Geol. J.* 57, 1912–1924. doi:10.1002/gj.4387

Zhang, K., Jiang, Z., Song, Y., Jia, C., Yuan, X., Wang, X., et al. (2022b). Quantitative characterization for pore connectivity, pore wettability, and shale oil mobility of terrestrial shale with different lithofacies -- A case study of the Jurassic Lianggaoshan Formation in the Southeast Sichuan Basin of the Upper Yangtze Region in Southern China. *Front. Earth Sci. (Lausanne).* 2022, 864189. doi:10.3389/feart.2022.864189

Zhang, K., Peng, J., Liu, W., Li, B., Xia, Q., Cheng, S., et al. (2020b). The role of deep geofluids in the enrichment of sedimentary organic matter: A case study of the late ordovician-early silurian in the upper yangtze region and early cambrian in the lower yangtze region, south China. *Geofluids* 2020, 1–12. doi:10.1155/2020/8868638

Zhang, K., Peng, J., Wang, X., Jiang, Z., Song, Y., Jiang, L., et al. (2020c). Effect of organic maturity on shale gas Genesis and pores development: A case study on marine shale in the upper yangtze region, south China. *Open Geosci.* 12 (2020), 1617–1629. doi:10.1515/geo-2020-0216

Zhang, K., Song, Y., Jia, C., Jiang, Z., Han, F., Wang, P., et al. (2022c). Formation mechanism of the sealing capacity of the roof and floor strata of marine organic-rich shale and shale itself, and its influence on the characteristics of shale gas and organic matter pore development. *Mar. Petroleum Geol.* 140 (2022), 105647. doi:10.1016/j.marpetgeo.2022.105647

Zhang, K., Song, Y., Jiang, Z., Xu, D., Li, L., Yuan, X., et al. (2022d). Quantitative comparison of Genesis and pore structure characteristics of siliceous minerals in marine shale with different TOC contents - a case study on the shale of Lower Silurian Longmaxi Formation in Sichuan Basin, Southern China. *Front. Earth Sci. (Lausanne).* 2022, 887160. doi:10.3389/feart.2022.887160

Zhang, K., Song, Y., Jiang, Z., Yuan, X., Wang, X., Han, F., et al. (2022e). Research on the occurrence state of methane molecules in post-mature marine shales-A case analysis of the Lower Silurian Longmaxi Formation shales of the upper Yangtze region in Southern China. *Front. Earth Sci. (Lausanne).* 2022, 864279. doi:10.3389/feart.2022.864279

Zhang, X., Ma, Y., He, J., Gong, C., and Wang, Y. (2021). Formation mechanism of high quality reservoir in glutenite:as an example of group Wuerhe at permian in Mahu area of Junggar Basin. *Inn. Mong. Petrochem. Ind.* 47 (08), 103–110.

Zhang, Z. (2019). *Oil-gas source correlation and migration tracing in the deep western central depression of Junggar Basin*. East China: China University of Petroleum. doi:10.27644/d.cnki.gsydu.2019.000134

Zhao, W., Hu, S., Guo, X., Li, J., and Cao, Z. (2019). New concepts for deepening hydrocarbon exploration and their application effects in the Junggar Basin, NW China. *Petroleum Explor. Dev.* 46 (05), 856–865. doi:10.1016/s1876-3804(19)60245-4

Zhi, D. (2016). Discovery and hydrocarbon accumulation mechanism of quasi continuous high efficiency reservoirs of Baikouquan Formation in Mahu sag, Junggar Basin. *Xinjiang Pet. Geol.* 37 (04), 373–382. doi:10.7657/XJPG20160401

Zhi, D., Tang, Y., Zheng, M., Guo, W., Wu, T., Zou, Z., et al. (2018). Discovery, distribution and exploration practice of large oil provinces of Above?Source conglomerate in Mahu sag. *Xinjiang Pet. Geol.* 39 (01), 1–8. doi:10.7657/XJPG20180101

Zhou, X., Huang, X., Wang, Q., Ma, Z., and Chen, L. (2020). Identification and description of the multi- stage sandy conglomerate fan body in Shinan Steep Slope Zone, Bohai Sea. *J. Northeast Petroleum Univ.* 44 (02), 46–55+8. doi:10.3969/j.ssn.2095-4107.2020.02.005

Zou, N., Zhang, D., Qian, H., Wu, T., and Shi, J. (2016). Main controlling factors of glutenite reservoir of fan delta in Mabei slope, Junggar Basin. *Lithol. Reserv.* 28 (04), 24–33. doi:10.3969/j.issn.1673-8926.2016.04.004

Zou, Z., Guo, H., Niu, Z., Yang, X., Xiang, S., Li, Y., et al. (2021). Sedimentary characteristics and controlling factors of river-dominated fan delta:a case study from the Upper Urho Formation in Mahu sag of Junggar Basin. *J. Palaeogeogr.* 23 (4), 756–770. doi:10.7605/gdlxb.2021.04.049